

Experimental and numerical investigations of controlled transition in low-speed free flight

Wolfgang Nitsche^{a,*}, Jörg Suttan^a, Stefan Becker^b, Peter Erb^c, Markus Kloker^d,
Christian Stemmer^d

^aInstitut für Luft- und Raumfahrt, Technische Universität Berlin, Marchstr. 12, 10587 Berlin, Germany

^bLehrstuhl für Strömungsmechanik, Universität Erlangen-Nürnberg, Cauerstr. 4, 91058 Erlangen, Germany

^cFachgebiet Strömungslehre und Aerodynamik, Technische Universität Darmstadt, Flughafenstr. 19, 64347 Darmstadt, Germany

^dInstitut für Aerodynamik und Gasdynamik, Universität Stuttgart, Pfaffenwaldring 21, 70550 Stuttgart, Germany

Received 13 June 2000; revised and accepted 19 March 2001

Abstract

This paper reports on the joint work of several university research groups, where scientists of five German universities tackled the problem of controlled laminar-turbulent transition on an unswept motor-glider wing with different low disturbance measurement methods on respective wing-gloves as well as with Direct Numerical Simulations. To establish a comparable measurement environment for the different measurement methods as well as to facilitate the comparison between measurement and numerical results, a controlled continuous disturbance wave train excited by a harmonic point source was introduced into the boundary-layer flow. A successful comparison between the controlled experiment and simultaneous computations is an essential step towards the understanding of more complex transition scenarios like natural transition. The investigation of the downstream development of the three-dimensional point-source disturbance was the main objective of the mutual research effort. © 2001 Éditions scientifiques et médicales Elsevier SAS

boundary layer / laminar-turbulent transition / harmonic point source / in-flight measurements / surface sensors / direct numerical simulation

Zusammenfassung

Experimentelle und numerische Untersuchung der kontrollierten Transition im Freiflug bei niederen Anströmgeschwindigkeiten. Die vorliegende Arbeit berichtet über Resultate aus Freiflugexperimenten und Direkter Numerischer Simulation im Rahmen eines kooperativen Forschungsprojektes zwischen mehreren Universitäten. Kontrollierte Experimente zum laminar-turbulenten Strömungsumschlag auf dem ungepfeilten Flügelhandschuh eines Motorseglers wurden mit Hilfe verschiedener störungsarmer Oberflächenmeßtechniken durchgeführt und mit Direkter Numerischer Simulation verglichen. Um eine Vergleichbarkeit zwischen den Experimenten und der Simulation zu gewährleisten, wurde ein kontinuierlicher Wellenzug durch eine harmonische Punktstörquelle in die Grenzschicht eingebracht. Erfolgreiche Vergleiche zwischen den kontrollierten Experimenten und der zeitgleichen Simulationen sind ein unverzichtbarer Schritt auf dem Weg zur Untersuchung und dem Verständnis komplexerer Umschlagsszenarien wie der freien Transition. Die Untersuchung der Stromabentwicklung des dreidimensionalen Wellenzuges war das Hauptziel des vorgestellten gemeinsamen Forschungsprojektes. © 2001 Éditions scientifiques et médicales Elsevier SAS

Grenzschicht / Laminar-Turbulente Transition / Harmonische Punktstörquelle / Freiflugmessungen / Oberflächensensoren / Direkte Numerische Simulation

* Correspondence and reprints.

E-mail addresses: Wolfgang.Nitsche@TU-Berlin.de (W. Nitsche), stemmer@iag.uni-stuttgart.de (Ch. Stemmer).

Nomenclature

CCA	constant current anemometer
c_x	streamwise phase velocity
\tilde{f}	dimensional disturbance frequency
h	multiple of the disturbance frequency
H_{12}	shape factor, $H_{12} = \delta_1/\delta_2$
IAS	Indicated Air Speed
k	multiple of the basic spanwise wavenumber
K	Kelvin
\tilde{L}	reference length scale
PVDF	Polyvinylidenfluoride
p	pressure
R	radius of the point source
Re	global Reynolds number
Re_{δ_1}	Reynolds number based on the local displacement thickness
SNR	Signal to Noise Ratio
\tilde{U}_∞	reference velocity
TAS	True Air Speed
u_e	normalised velocity at the boundary layer edge
u, v, w	velocity in the streamwise, wall normal, spanwise direction
x, y, z	streamwise, wall normal, spanwise direction
α	angle of attack
α_r	streamwise wavenumber
β	angle of yaw
γ	basic spanwise wavenumber
δ	boundary-layer thickness ($u = 99\% \tilde{U}_\infty$)
δ_1	boundary-layer displacement thickness
δ_2	boundary-layer momentum thickness
λ_z	spanwise width of the integration domain
$\tilde{\nu}$	kinematic viscosity
θ	obliqueness angle of disturbance waves with respect to the x -direction
$\omega_x, \omega_y, \omega_z$	vorticity in the streamwise, wall normal, spanwise direction
<i>subscripts</i>	
B	baseflow quantities
rms	root-mean-square
<i>superscripts</i>	
'	disturbance quantities
~	dimensional quantities

1. Introduction

The DFG university research group, with the participating universities from Aachen, Berlin, Darmstadt, Erlangen and Stuttgart, conducted a joint research project on laminar-turbulent transition in free flight during the last years. This project continues the efforts begun in the late 1980s [3].

The objective of the joint research effort was to examine the temporal and spatial development of a boundary-layer transition under low-disturbance free-flight conditions and to compare the measurement results with accompanying direct numerical simulations. The experi-

mental groups employed different low-disturbance high-resolution measurement methods such as multi-sensor hotfilm, piezofoil arrays, and a miniaturised LDV probe. The numerical simulation project solved the complete unsteady three-dimensional Navier–Stokes equations in the area of an adverse pressure gradient up to the turbulent flow regime. As a common test case, the development of a three-dimensional wave train excited by a harmonic point source in the boundary layer of the wing was examined by all members of the research group. This represents a vital step towards the investigation and understanding of natural transition in free-flight and the comparison to uncontrolled transition in wind-tunnel experiments.

2. Experimental aircraft and flight measurement systems

As a test aircraft, the Grob G109b motorglider of the TU Darmstadt was employed. This aircraft provides ample space as well as payload capacity. Measurements can be performed while soaring, i.e. with the engine switched off, to reduce disturbances due to engine noise or engine induced vibrations. The aircraft is equipped with a flight-data measurement system which continuously measures and calculates the flight attitude data (α , β , TAS, Re) as well as air data (temperature, humidity, pressure). The data is stored on a hard disk for further examination and is also visible on a flight guidance instrument in the cockpit. The flight attitude can be monitored during the flight to enable the pilot to hold a predefined attitude setting for the required measurement time (figure 1, see also Erb et al. [2]). It could be verified that the attitude setting could be held for adequate time periods to perform the multisensor and LDV measurements at an accuracy of $\Delta\alpha_S = \pm 0.05^\circ$.

On the starboard wing of the aircraft, provisions are made for the mounting of a laminar wing glove (compare figure 2 with the indicated integration domain for the DNS calculations). Each experimentally working project

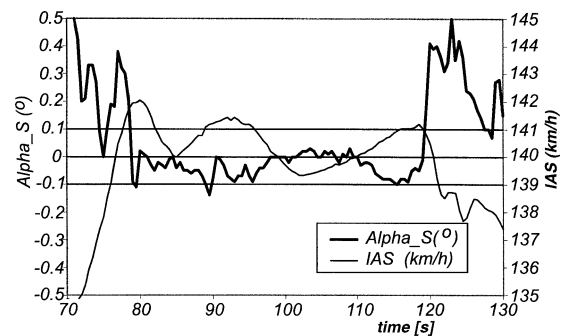


Figure 1. Excerpt from the data acquisition system on board the aircraft. The angle of attack α_S can be controlled to $\Delta\alpha_S = \pm 0.05^\circ$.

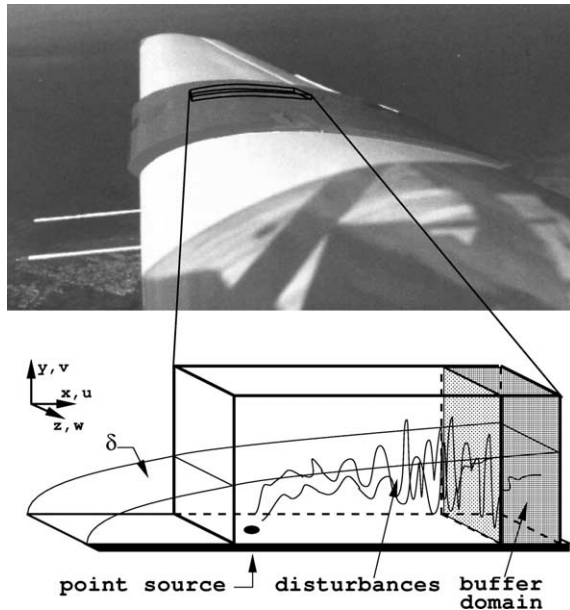


Figure 2. Wing glove mounted on the aircraft and integration domain for the Direct Numerical Simulations.

group employs their own glove equipped with the special measurement systems. The gloves were uniformly built by the same group in the same mould. The gloves could be mounted on the motorglider wing without compromising the aircraft structure. Measurement equipment could be mounted in an under-wing pod adjacent to the wing glove as well as on a shock- and vibration damped platform behind the pilot seats. All wing gloves are equipped with the harmonic point source (see figure 3). A ceramic

insert with six discrete circularly-arranged holes is flush-mounted with the surface of the gloves. The arrangement of multiple hole was chosen to minimize unwanted noise and to inhibit nonlinear effects in comparison to a one-hole arrangement, as it was employed e.g. in Gaster's wave packet experiments [4]. The insert is located at the centre of the glove at a downstream position of $x/c = 0.27$. The ceramic insert is connected to a loudspeaker in the under-wing pod by means of a pressure tube. The loudspeaker itself is mounted in the wing pod and is driven by a computer controlled sine wave generator. To ensure comparability of the measurement results, the disturbance output can be equalised prior to the flight by means of a p' -sensor. Various independent in-flight measurements of low-amplitude u'_{rms} -profiles allowed for the adjustment of the simulated parameters (for a detailed description about the matching of experimental settings with simulation parameters, please refer to [5]).

3. Experimental and numerical methods

The in-flight measurements and the accompanying windtunnel pre-tests were carried out with a variety of modern low-disturbance measurement methods. For the measurement of surface force fluctuations, multisensor piezofoil- and hotfilm-arrays were employed, while for measurements inside the boundary layer above the wing glove surface, a miniature LDV-probe was used. A special hot wire probe was used to measure wall-normal profiles of the streamwise velocity disturbances to ensure matching of simulations and measurements. Details about comparisons between in-flight measurements and windtunnel tests are to be found in [6].

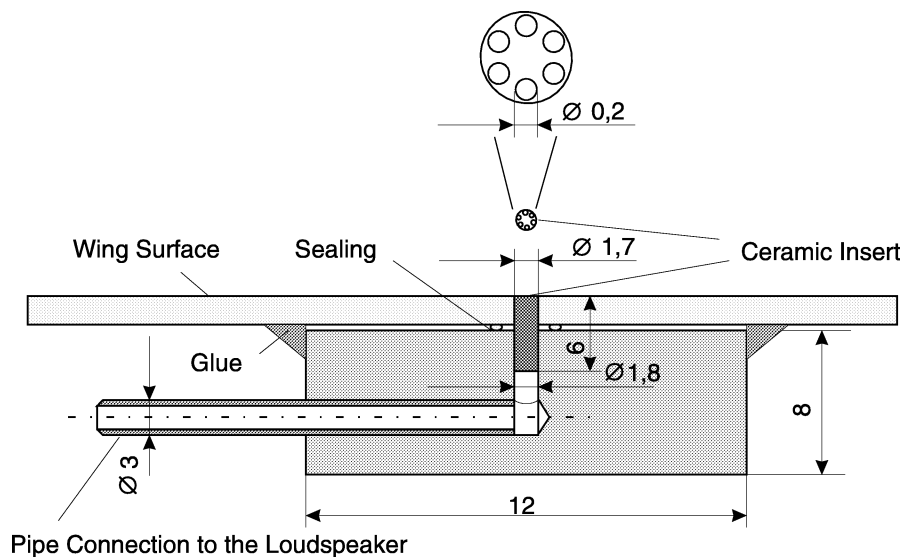


Figure 3. Layout of the disturbance source.

3.1. Multi-sensor piezofoil arrays

Sensors or sensor arrays made of piezoelectric foil material (Polyvinylidenfluoride, PVDF) have been used for the measurement of unsteady surface forces (the sensors are sensitive to pressure and shear [9]) for several years now. Since piezofoils are very thin and flexible they can be flush-mounted on almost all surfaces. A piezofoil sensor consists of a PVDF-layer which is covered with metallic layers on both sides. By partially removing the metallic layer on the lower side of the foil, it is possible to create multi-sensor arrays which are customised for a given measurement case. The number of sensors is only limited by the capabilities of the related data acquisition system while the sensor size and spacing depends on the necessity to obtain a sufficient signal-to-noise-ratio (SNR). By means of applying a small temperature gradient between the surface of the wing glove and the flow ($\sim 2\text{ K}$), it is possible to increase the signal amplitude as well as the SNR significantly (Sturzebecher and Nitsche [9]) and hence minimize the necessary sensor size. Two piezofoil sensor arrays with 192 discrete sensors each which were used for the in-flight measurements are shown in *figure 8(a)*. The first (upper part of the sketch) delivered the downstream evolution of the wave train over a lengthy distance, whereas the second (lower part of the sketch) was used for more detailed results in the transitional regime. A custom-designed digital multi-channel measurement system was employed.

3.2. Multi-sensor hotfilm arrays

Two experimental groups from the RWTH Aachen and from the TU Darmstadt employed multi-sensor surface hotfilm arrays to measure shear stress fluctuations on the wing glove. The RWTH Aachen developed different arrays with up to 168 sensors and they were tested during different measurement campaigns. The size of the sensors as well as the spacing was minimized during the research project, the smallest sensors having a size of $0.750\text{ mm} \times 0.0080\text{ mm}$ with a spanwise spacing of 2.35 mm (*figure 9(a)*). The 108 sensor array shown was designed such that at three different downstream positions, a double spanwise row of sensors was mounted. This offered the possibility to determine downstream (as well as streamwise) wave numbers at these distinct locations. The necessary anemometer was operated in constant current (CCA) mode, thus reducing the number of necessary connector lines. The anemometers were connected to a 96-channel data recorder with a maximum sampling frequency of 50 kHz per channel. The TU Darmstadt, following a different approach, developed a sensor array with only 32 sensors aligned in the streamwise direction. To capture the 3-D-development of the artificial excitation, the point source was mounted in a carriage which could be traversed in spanwise direction

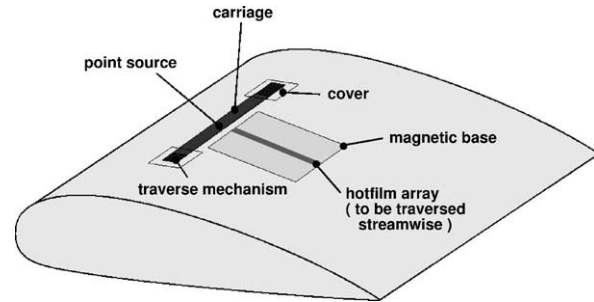


Figure 4. Sketch of the layout of the hotfilm array and the point source traverse mechanism of the TU Darmstadt.



Figure 5. LDV probe during in-flight tests.

during flight. To reach a higher streamwise resolution, the sensor array itself was mounted on a magnetic plate and could be positioned at different downstream positions on the wing glove (*figure 4*). Thus, the spacing was $1.5\text{ mm} \times 2.25\text{ mm}$ in spanwise/downstream direction. By also recording the disturbance signal, a phase-equal signal analysis could be performed even for different flight tests.

3.3. Miniature LDV probe

The University of Erlangen-Nürnberg developed a miniature LDV-Probe which could be mounted in the small gap between the wing surface and the wing glove skin. Through this arrangement, only two small mirrors are protruding into the flow (*figure 5*). The optical and measurement system is described in more detail in Becker et al. [1]. The very heavy measurement equipment made it necessary to automate the measurement and data acquisition in such a way that it could be operated by the pilot alone, saving the weight of the measurement engineer.

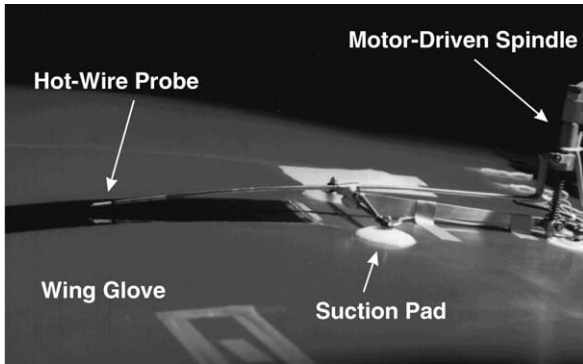


Figure 6. Hotwire probe (TU Berlin) for disturbance velocity measurements mounted on the wing glove.

3.4. Special hotwire probe

To perform a detailed analysis of the behaviour of the wave train emanating from the harmonic point source under free flight conditions, a special hotwire probe was developed by the TU Berlin (*figure 6*). Mounted in a protruding beam, a commercially available hotwire probe (TSI) could be traversed perpendicular to the wing glove surface through the boundary layer to obtain velocity as well as disturbance profiles.

3.5. Numerical procedure

In the simulations, the complete unsteady three-dimensional Navier–Stokes equations in vorticity-velocity formulation are solved in a fixed rectangular box on the surface. The surface curvature is neglected but the full streamwise variation of the base flow is included in the spatial simulation model. A finite-difference scheme, fourth order accurate in time and space, is employed. The spanwise direction is discretised using Fourier modes exploiting periodic boundary conditions. At the upper box boundary, the boundary-layer edge velocity gained from in-flight measurements is prescribed. The harmonic point source (HPS), experimentally set up by a circle of holes on the glove surface with a loudspeaker underneath, is modelled in the DNS by timewise periodic simultaneous blowing and suction with a one-hole area at the wall. The detailed numerical procedure and some spatial results are extensively described in [5,7,8].

4. Experimental results

In this section, some results gained by the different measurement techniques will be presented. Results of the combined numerical and experimental investigations are presented in section 5.

By means of the 192-sensor piezofoil array it was possible to measure the amplification of the artificially induced disturbance wave in a large area of the wing

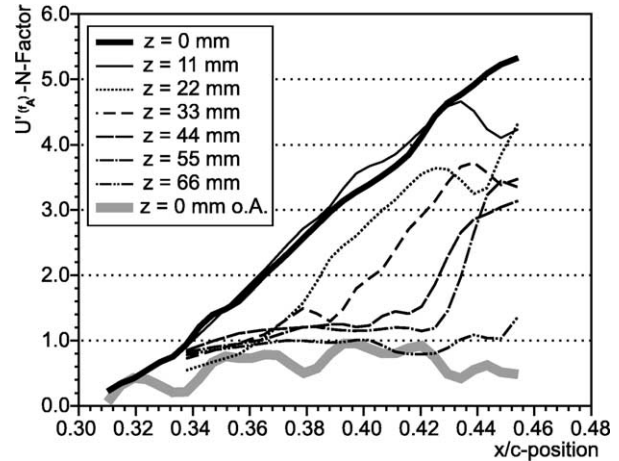


Figure 7. N-factors from piezofoil measurements at different spanwise positions with the HPS-excitation and at the centreline without excitation (o.A.). Data from the TU Berlin.

glove surface in one measurement. *Figure 7* shows relative N-factors $N = \ln(A_{(x/c)}/A_{(x/c=0.3)})$. Due to the three-dimensional expansion of the wave train, the increase of signal amplitude can be seen at first on the sensor rows immediately downstream of the point source ($z = 0–11$ mm). The outer sensor rows show the increasing spanwise extension of the wave train ($z = 22, 33, 44, 55$ mm respectively). At $z = 66$ mm, the signal amplitude is almost equal to that of the undisturbed flow.

A different representation of the process can be seen in the plots of isosurfaces of instantaneous signal amplitudes in *figure 8(b)*. Downstream of the point source, the characteristic half-moon shaped wavefronts of the three-dimensionally developing wave train can be seen. Further downstream, the strong amplification and finally breakdown of the waves is visible along with a strong spanwise variation of signal amplitude. The lower picture shows the benefits of the increased spatial resolution ($6 \text{ mm} \times 6 \text{ mm}$ compared to $6 \text{ mm} \times 11 \text{ mm}$ in the upper picture) in spanwise direction. In the core region of the disturbance wedge, distinct structures can be observed. Their origin will be clarified in section 5.

A similar behaviour can be derived from the surface hot-film signals measured with the 96-sensor array of the RWTH Aachen. *Figure 9(b)* shows isolines of signal phase at the three different sensor positions (compare with *figure 9(a)*). Here, the increasing spanwise perturbation of the 3-D-wave can also be seen. The strongly three-dimensional nature of the boundary layer excitation can be derived from *figures 10(a)* and *(b)*.

Figure 10(a) shows the relation between streamwise and spanwise wavenumber α_r and γ respectively. With increasing spanwise wavenumber γ the streamwise wavenumber α_r first decreases in the region of linear amplification as was predicted from wind tunnel pre-tests. The streamwise component of phase velocity c_x decreases

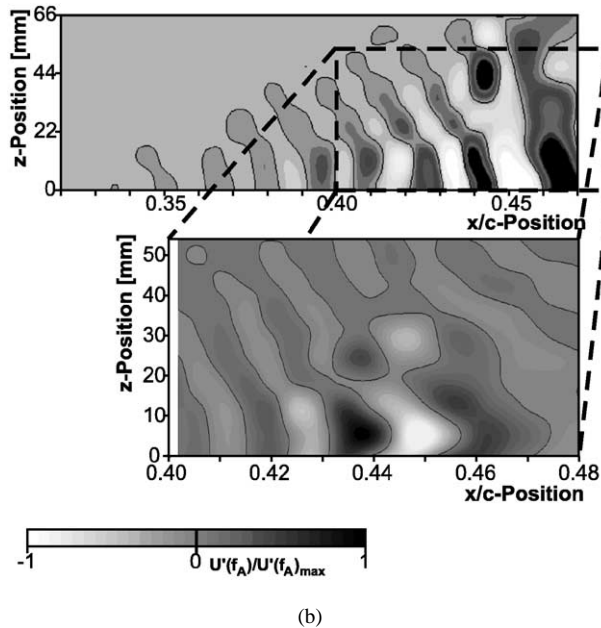
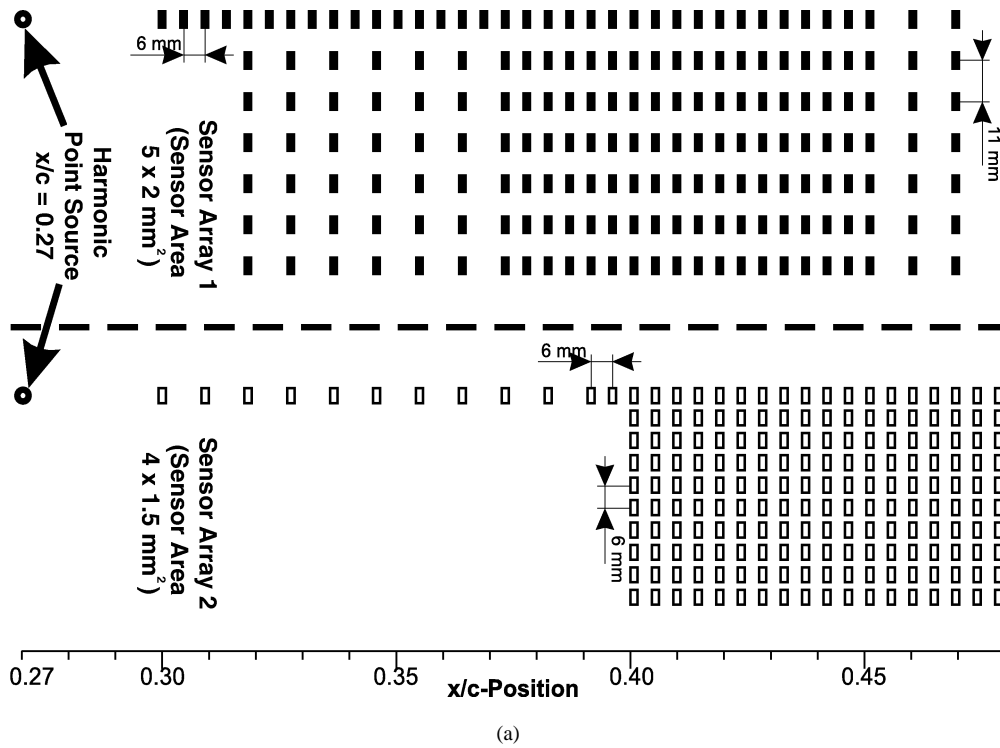


Figure 8. Measurement setup and results by the TU Berlin: (a) layout of the piezofilm arrays used by the TU Berlin; (b) iso-surfaces of the instantaneous signal amplitudes from piezofilm measurements of the TU Berlin (array 1 and array 2).

continuously with increasing spanwise wavenumbers γ for large spanwise wavenumbers c_x reaches very low values as could be expected due to the large angle of the oblique waves (*figure 10(b)*).

As an example for the results from the hotfilm measurements of the TU Darmstadt, time traces and Fourier spectra of the sensor signals are shown in *figure 11*. The time traces show the development of the artificial excita-

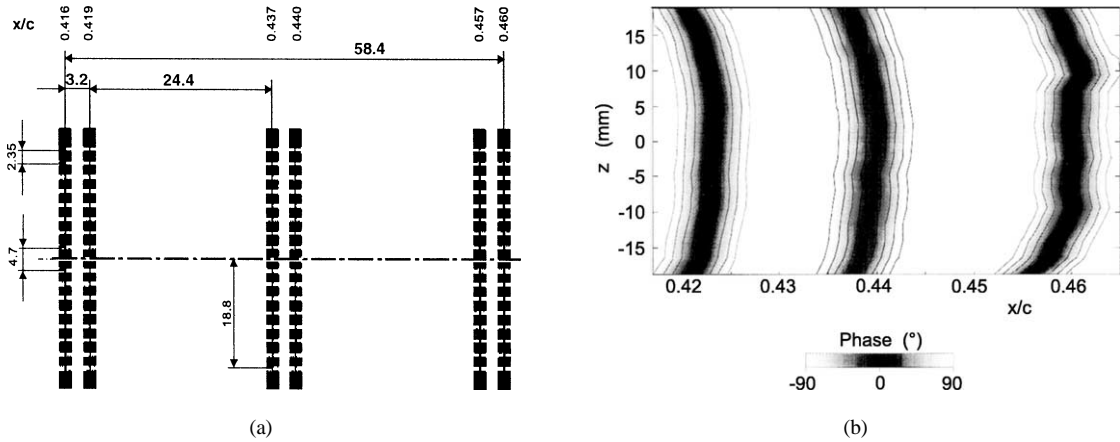


Figure 9. Measurement setup and results by the RWTH Aachen: (a) layout of the hotfilm array used by the RWTH Aachen; (b) lines of equal phases.

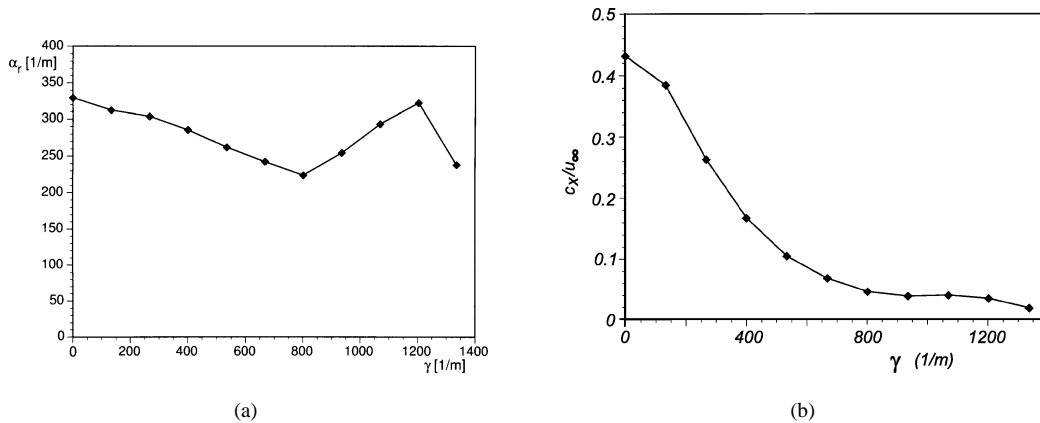


Figure 10. Wavenumbers from RWTH Aachen: (a) streamwise wavenumber; and (b) streamwise phase speed versus spanwise wavenumber at $x/c = 0.437$.

tion wave (represented by the timetrace at $x = 350 \text{ mm} \hat{=} x/c = 0.27$). Starting with $x = 440 \text{ mm} \hat{=} x/c = 0.34$, the excitation frequency can clearly be distinguished in the time traces. The increase in wave amplitude is accompanied by an overlapping increase of the higher harmonic frequencies, simultaneously visible in the time-traces ($x = 520\text{--}530 \text{ mm} \hat{=} x/c = 0.40$) as well as in the Fourier spectra. Downstream of $x = 550 \text{ mm} \hat{=} x/c = 0.423$ the amplitude of the fundamental frequency decreases and thus shows the laminar-turbulent transition.

In addition to the wall-bound measurement techniques, the special hotwire probe from TU Berlin as well as the LDV measurements from the University Erlangen-Nürnberg delivered an insight into the flow field above the surface. For different disturbance amplitudes, profiles of the downstream velocity U (figure 12) and the disturbance velocity u' were derived from the hotwire measurements at $x/c = 0.375$. It is visible that, while the velocity profiles still show a laminar shape, the disturbance

amplitudes may reach levels above $u' = 1\%$, which is associated with non-linear excitation amplitudes.

Figure 13 shows the characteristic shape of boundary layer velocity profiles in the laminar (figure 13(a)) as well as in the turbulent (figure 13(b)) boundary layer measured with the miniature LDV probe.

5. Comparison of experimental and numerical results

The hotwire measurements provided disturbance profiles of the downstream velocity u' (figure 14). After the DNS was adjusted for the disturbance amplitude of the point source, the shape of the wall-normal velocity profile coincides almost perfectly with the measured data acquired from three different flights. The time traces and the spectra are shown for different distances normal to the wall as well in figure 14. This provides the foundation for the comparability of the simulations with the various measurements.

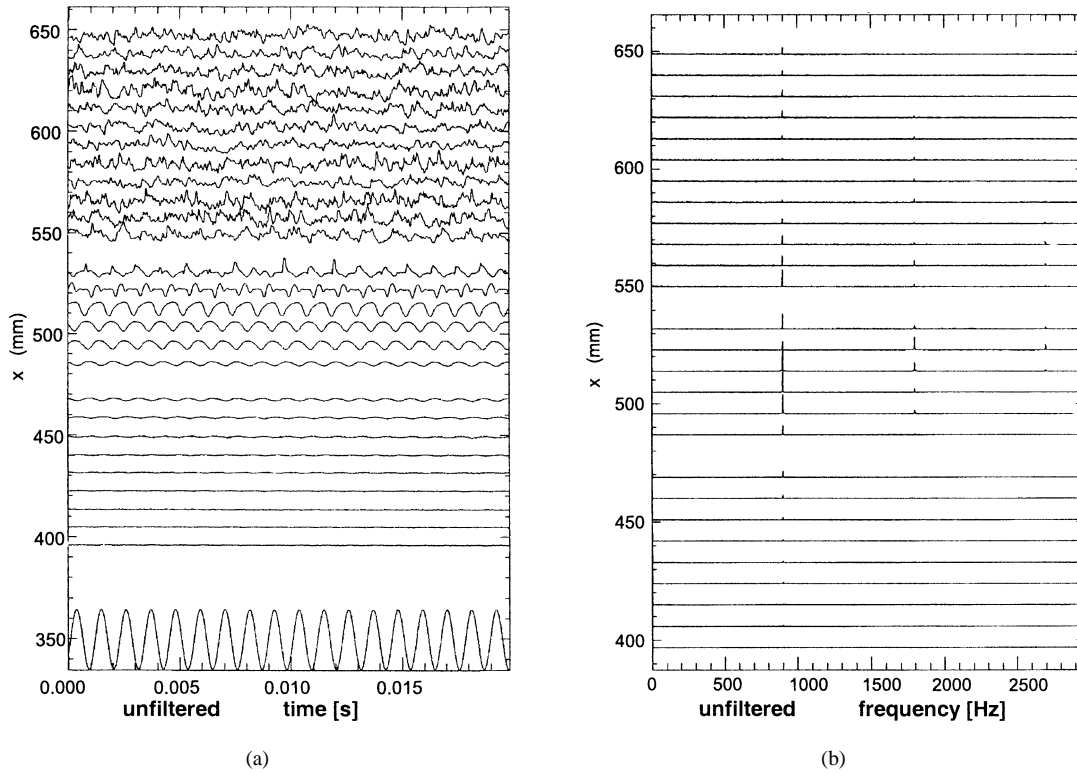


Figure 11. Hotfilm measurements by the TU Darmstadt: (a) time traces; (b) Fourier spectra.

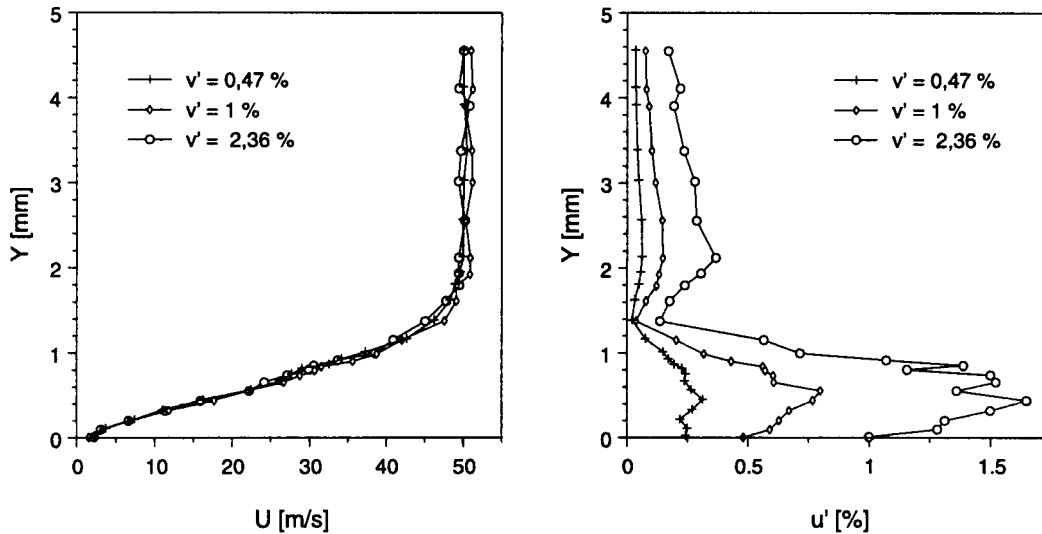


Figure 12. Velocities measured via hotwire by the TU Berlin. left: velocity profiles; right: disturbance profiles for different disturbance levels.

The comparison of disturbance profiles (u'_{rms} at $z = 20$ mm) from DNS and LDV measurements falls short of the previously shown hotwire comparisons (figure 15). The already quite advanced measurement position at $x/c = 0.425$, where transition is almost complete, explains some of the diverging results at the already non-linear disturbance amplitudes of $u' = 3$ m/s. The devel-

opment close to the wall seems to be difficult to be measured by the LDV setup. The development for $y > 1$ mm shows good agreement as well as the wall-normal location of the maximum amplitude. Close to the wall, the data rate for the LDV measurements drops considerably and the SNR goes up.

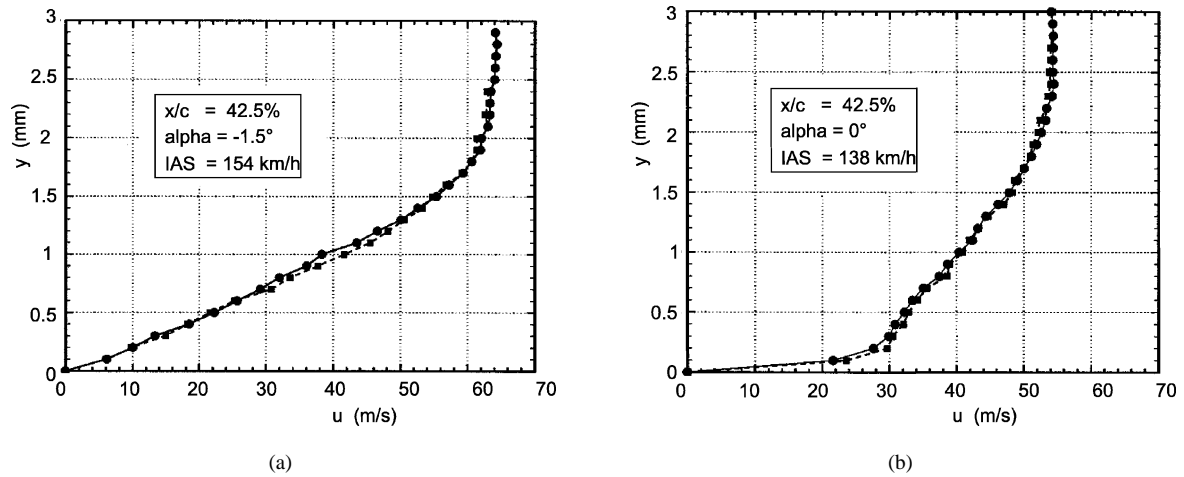


Figure 13. LDV measurement from the Universität Erlangen-Nürnberg: (a) laminar profile; (b) turbulent profile.

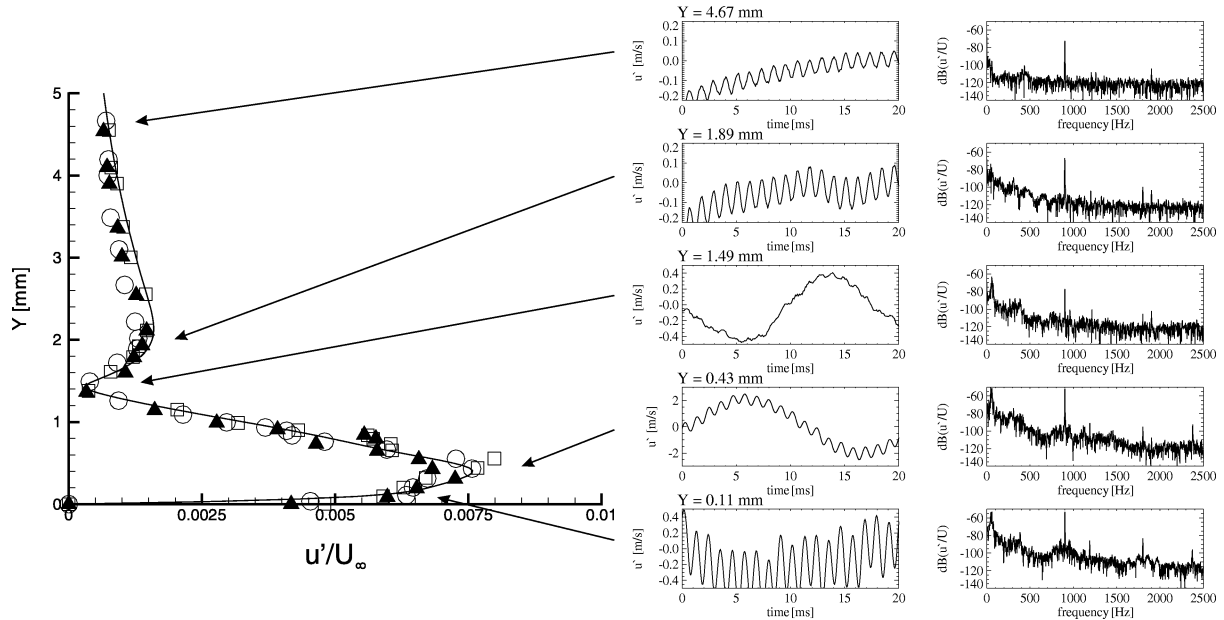


Figure 14. Hotwire measurements by the TU Berlin compared to the DNS u'_{rms} values at $x/c = 0.37$.

The comparison of the assembled hotfilm data acquired by the TU Darmstadt with respective DNS data of the instantaneous spanwise vorticity ω'_z is shown in figure 16. The measurements are filtered such that the steady part of the hotfilm signal is not represented. The measurement technique is not able to distinguish between reversed flow and streamwise flow, rather, frequency doubling is obtained for instantaneous reversed flow. The wave train in its spatial linear development is clearly captured by both measurement and simulation. The footprints of a developing pair of Λ -vortices can be identified in both representations at $z/c = \pm 0.0075$ and $x/c = 0.41$ as a

deformation of the bow-shaped wave front to an M-shape structure. The spatial extension of the Λ -vortices inside the boundary layer is shown in detail in [8]. A turbulent spot develops downstream of $x/c = 0.42$ with very high unsteady vorticity ω'_z at the wall (steady shares of the base flow vorticity and the time average mean are removed from the signal). At the sides of the turbulent spot, the outward pointing ends of the wave fronts persist for a surprisingly long time which is captured in the measurements.

The surface measurements from the TU Berlin show the same nonlinear behaviour as the DNS and the hot-

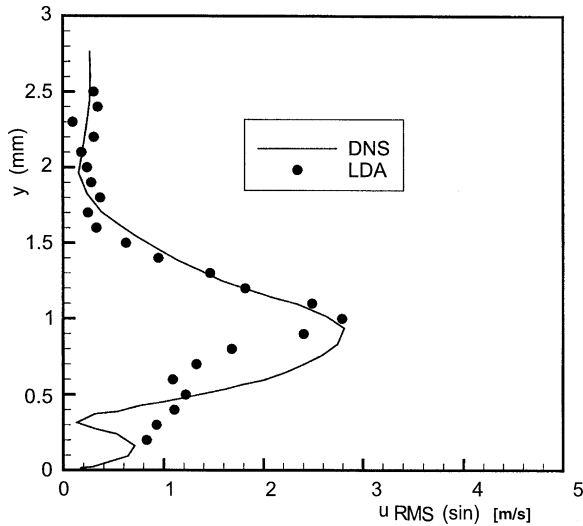


Figure 15. The disturbance rms velocity profiles as measured by the LDV probe through the Universität Erlangen-Nürnberg group compared to the respective DNS u'_{rms} data for $x/c = 0.425$ and $z = 20$ mm for the frequency $\tilde{f} = 900$ Hz.

film measurements, although, admittedly, further downstream. The M-shape structure at the wall, first described in the DNS [5], is clearly identifiable from the measurements. Detailed further comparison with piezofoil data acquired by the TU-Berlin group can be found in [6].

6. Conclusions

The presented results from hotfilm and piezofoil surface measurement techniques and hotwire and LDV measurements with DNS show a comprehensive picture of the transition of a harmonic point source disturbance in an airfoil boundary-layer flow. The described measurement techniques were adapted to the free-flight conditions and were successfully employed in-flight. It could be shown that the different high resolution measuring techniques are truly capable of detecting transitional behaviour of the highly three-dimensional wave train breakdown. Hotfilm and piezofoil measurements are able to detect Λ -vortex footprints as the measurement results are compared with DNS results showing the spatial developments of a staggered pattern of Λ -vortices.

Acknowledgements

The authors as well as all the participants of the joint university research group gratefully acknowledge the financial support for their work by the DFG (German Research Foundation) through grants Be 1192/5, Du 101/30, Ew 17/10, Kr 387/26, Ni 282/7 and Ni 282/8).

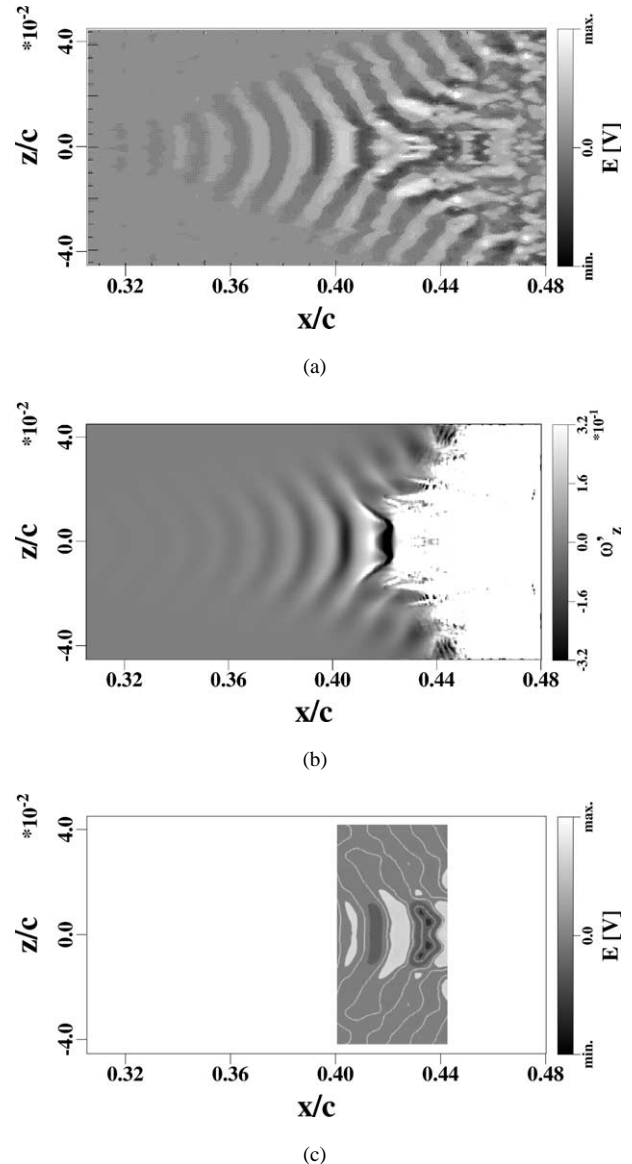


Figure 16. Comparison of (a) instantaneous hotfilm disturbance signals by the TU Darmstadt with (b) instantaneous spanwise vorticity ω'_z at the wall (steady part removed) from DNS and (c) instantaneous piezofoil sensor signals from the TU Berlin.

References

- [1] Becker S., Durst F., Lienhart H., Laser Doppler anemometer for in-flight velocity measurements on airplane wings, *AIAA J.* 37 (6) (1999) 687–690.
- [2] Erb P., Ewald B., Roth M., Flight experiment guidance technique for research on transition with Grob G109 aircraft of the Technische Hochschule Darmstadt, in: Körner H., Hilbig R. (Eds.), *Notes on Numerical Fluid Mechanics*, 60, Vieweg Verlag, Wiesbaden, 1997, pp. 143–150.

- [3] Ewald B., Durst F., Krause E., Nitsche W., In-flight measuring techniques for laminar flow wing development, *Z. Flugwiss. Weltraum.* 17 (5) (1993) 294–310.
- [4] Gaster M., The nonlinear phase of wave growth leading to chaos and breakdown to turbulence in a boundary layer as an example of an open system, *P. Roy. Soc. Lond. A* 430 (1990) 3–24.
- [5] Stemmer C., Kloker M., Wagner S., DNS of Harmonic Point Source Disturbances in an Airfoil Boundary Layer, AIAA Paper 98-2436, 1998.
- [6] Stemmer C., Suttan J., Kloker M., Nitsche W., Point-source induced transition in free flight, in: Nitsche W., Heinemann H.-J., Hilbig R. (Eds.), *Notes on Numerical Fluid Mechanics*, 72, Vieweg Verlag, Wiesbaden, 1999, pp. 458–465.
- [7] Stemmer C., Kloker M., Later stages of transition of an airfoil boundary layer flow excited by a harmonic point source, in: Fasel H., Saric W. (Eds.), *Laminar-Turbulent Transition*, Springer Verlag, Berlin, Heidelberg, 2000.
- [8] Stemmer C., Kloker M., Wagner S., Navier–Stokes simulation of harmonic point source disturbances in an airfoil boundary layer, *AIAA J.* 38 (8) (2000) 1369–1376.
- [9] Sturzebecher D., Nitsche W., Visualisation of the spatial-temporal instability wave development in a laminar boundary layer by means of a heated PVDF sensor array, in: Körner H., Hilbig R. (Eds.), *Notes on Numerical Fluid Mechanics*, 60, Vieweg Verlag, Wiesbaden, 1997, pp. 335–342.